

Lidar temperature series in the middle atmosphere as a reference data set. Part 2: Assessment of temperature observations from MLS/Aura and SABER/TIMED satellites

Robin Wing¹, Alain Hauchecorne¹, Philippe Keckhut¹, Sophie Godin-Beekmann¹, Sergey Khaykin¹, and Emily M. McCullough²

¹LATMOS/IPSL, UVSQ Université Paris-Saclay, Sorbonne Université, CNRS, Guyancourt, France

²Department of Physics and Atmospheric Science, Dalhousie University, Halifax, Canada

Correspondence to: Robin Wing (robin.wing@latmos.ipsl.fr)

Abstract. We have compared 2433 nights of Rayleigh lidar temperatures measured at L'Observatoire de Haute Provence (OHP) with co-located temperature measurements from the Microwave Limb Sounder (MLS) and the Sounding of the Atmosphere by Broadband Emission Radiometry instrument (SABER). The comparisons were conducted using data from January 2002 to March 2018 in the geographic region around the observatory (43.93° N, 5.71° E). We have found systematic differences between the temperatures measured from the ground based lidar and those measured from the satellites which suggest non-linear distortions in the satellite altitude retrievals. We see a winter stratopause cold bias in the satellite measurements with respect to the lidar (-6 K for SABER and -17 K for MLS), a summer mesospheric warm bias (6 K near 60 km), and a vertically structured bias for MLS (-4 to 4 K). We have corrected the stratopause height of the satellite measurements using the lidar temperatures and have seen an improvement in the comparison. The winter relative cold bias between the lidar and SABER has been reduced to 1 K in both the stratosphere and mesosphere and the summer mesospheric warm bias is reduced to 2 K. Stratopause altitude corrections have reduced the relative cold bias between the lidar and MLS by 4 K in the early autumn and late spring but were unable to address the apparent vertical oscillations in the MLS temperature profiles.

1 Introduction

Satellite atmospheric measurements are vital for providing global assessments of long term atmospheric temperature trends. However, particular care must be taken to validate each new satellite as well as provide periodic ground checks for the entire instrument lifetime in order to counter drifts in calibration and local measurement time (Wuebbles et al., 2016). Changes in satellite measurements

can occur over the course of a mission due to instrument degradation, calibration uncertainties, orbit changes, and errors/assumptions in the forward model parameters. Additionally, most mission planning agencies have guidelines which require that satellite programs conduct formal validation studies to ensure accuracy and stability of the measurements (Council, 2007).

25 1.1 Lidar as a Validation Tool

Rayleigh lidar remote sounding of atmospheric density and temperature is an excellent tool for use in validating satellite measurements over a specified geographic area and vertical range. Lidars can make routine high resolution measurements over a large portion of the middle atmosphere in regions which are notoriously difficult for other techniques to measure routinely or precisely. There are two
30 key strengths in the Rayleigh lidar technique which set it apart from other atmospheric sounders.

First is the ability to retrieve an absolute temperature profile from a measured relative density profile with very high spatio-temporal accuracy and precision.

Second, lidars measure range by measuring the time required for a backscattered photon to return to the station and be recorded by the photon counting electronics. The current OHP lidar uses a Licel
35 digital recorder and has a sampling 40 MHz which corresponds to a vertical resolution of 7.5 m. The uncertainty on the sampling rate is negligible however, there is the possibility of trigger delay and jitter in the counting electronics of 50 ± 12.5 ns Licel (2018) contributing a maximum possible uncertainty of 18.25 ± 3.25 m in the raw lidar measurement. This error is constant with altitude which allows us to sample the upper middle atmosphere with the same range resolved confidence as the
40 lower middle atmosphere and troposphere. In contrast, passive remote sensors such as limb scanning satellites can suffer biases at high altitudes due to: radiometric and spectral calibration, field of view and antenna transmission efficiency, satellite pointing uncertainty, as well as biases introduced by the forward model (Schwartz et al., 2008). Additionally, many satellites like MLS are optimized for tropospheric and lower stratospheric measurements and conduct faster scans with fewer channels at
45 higher altitudes (Livesey et al., 2006). These different biases can exist simultaneously in both the retrievals of temperature and pressure and can be considered, in part, as distortions in the altitude vector when compared to lidar measurements.

1.2 Previous Lidar-Satellite Temperature Studies

Previous studies comparing ground based lidar and satellite measurements of temperature have often
50 used Sodium Resonance lidars to compare the lidar derived neutral temperature between 85 km and 105 km to satellite temperatures in the mesopause region. Studies of this sort have generally shown good agreement between ground and satellite observations (Xu et al., 2006). Due to the strength of Na lidars in the upper mesosphere they naturally lend themselves well to studies of tides and wave breaking dynamics.

55 Coincident with this work (Dawkins et al., 2018) submitted a comparison of temperature profiles
from 9 different metal resonance lidars with temperature profiles from SABER from 75 to 105 km.
At all sites they found that SABER temperatures were cooler than the lidar temperatures by -9.9
(±9.7) K at 80 km. The study used coincidence criteria of $\pm 15^\circ$ longitude, $\pm 5^\circ$ latitude, and ± 30
60 minutes between the lidar and satellite profiles. A weak and unexplained mesospheric summer bias
was also reported. In the supplemental material to (Dawkins et al., 2018) a sensitivity study was
done for SABER overpasses as a function of season and size of the co-location area. They found no
significant differences between a co-location area with a longitudinal size of $\pm 5^\circ$ and $\pm 15^\circ$.

A study by (Yuan et al., 2010) compared Na lidar and SABER temperatures in the context of a 6
year tidal analysis. They found semiannual disagreements in the tidal amplitude around the spring
65 and autumn equinoxes with a maximum difference of 12 K near 90 km occurring in February. Several
explanations and partial corrections were offered but the phenomenon is robust and the authors con-
cluded that further study was required to fully resolve the temperature discrepancy. Studies have also
been done comparing temperatures calculated from the Rayleigh lidar technique and those derived
from SABER and MLS observations. (Taori et al., 2011, 2012a, b) comprise an excellence series
70 of publications using multiple instruments to measure the atmospheric temperature from 40 km to
100 km. These works found good agreement between the lidar and SABER up to 65 km and signif-
icant initialization errors in the lidar of up to 25 K near 90 km. We have partially accounted for this
initialization induced lidar warm bias in the companion paper (Wing et al., 2018). Our work here
offers two improvements on these three publications. Firstly, we have not focused as much on case
75 studies but rather on the statistics of nearly a decade of lidar-satellite inter-comparisons. Secondly,
we have conducted our comparisons on a 1 km grid in an effort to match small scale features in the
temperature profiles.

A good lidar to satellite temperature comparison was done by (Siva Kumar et al., 2003) using
240 nights of lidar temperatures, temperatures from UARS, and model temperatures from CIRA-
80 86 and MSIS-90. They compared monthly and seasonal averages and found significant semiannual
temperature anomalies in the region of 45 – 50 km in February-March and September-October as
well as initialization related biases above 70 km. A second study by the same authors compared 14
years of monthly average lidar temperatures to temperatures from the satellites SABER, HALOE,
COSMIC, and CHAMP (Sivakumar et al., 2011). As with the previous study temperature anomalies
85 of 3-5 K were identified in the region near the stratopause. The differences were attributed to monthly
averaging and slight differences in measurement time and location of the lidar and satellites. The
approach employed in our work is to make comparisons of nightly averages and then study the
monthly median of the temperature differences – an approach which will allow for finer temporal
precision.

90 Another study which compares 120 nights of Rayleigh lidar temperatures measured over Beijing
to temperatures from SABER over the course of one year found good agreement between monthly

average temperature profiles (Yue et al., 2014). This study found winter time temperature anomalies in the stratopause region and attempted to account for these features by fitting an annual, semi-annual, and 3 month sinusoid to the data. The objective of our study is similar to that of Yue et al. (2014) insofar as we are interested in the time evolution of lidar-satellite temperature comparisons and identifying potential seasonal or decadal trends. However, we are seeking to make nightly temperature comparisons between lidar and two satellites, SABER and MLS, over multiple years without assuming large contributions from an Annual Oscillation (AO) or its harmonics. Our study uses more than 9 times as many coincident measurements and spans the entire SABER data record.

Further study of seasonal temperature anomalies between ground based lidar and SABER was done by (Dou et al., 2009) comparing 2332 nights of lidar data from 6 different sites in the Network for the Detection of Composition Change (NDACC) to zonally averaged temperature profiles from SABER. This study found a 2-5 K systematic bias in the stratopause region and concluded that this result may be due to either a bias in SABER, tidal aliasing, or sporadic aerosols. As well the study found systematic temperature differences in the upper mesosphere which were attributed to tidal aliasing, bias in the SABER temperature retrieval, or temperature differences due to the AO. In our work we use a smaller geographic window and not a zonal average temperature to compare more truly co-incident measurements. As well we limit the time difference between the lidar and satellite measurements to minimize possible tidal contributions.

1.3 Alternative Measurement Techniques

Other current measurement techniques for atmospheric temperature in this region of the atmosphere include:

a) Rocketsondes were used during the early satellite era to make in situ measurements of the middle atmosphere but this technique has many well known limitations and requires large corrections and uncertainties in the upper mesosphere (Johnson and Gelman, 1985).

b) Meteor radar techniques provide an estimation of the temperature at 90 km and can operate on a near continuous basis but they require several a priori assumptions and must be calibrated with data from an independent source (Meek et al., 2013)

c) Satellites, like MLS and SABER provide globally distributed temperature measurements at several pressure levels throughout the vertical atmospheric column (Waters et al., 2006) (Mertens et al., 2001). Satellite based measurements provide a very good global view of the Earth's middle atmosphere but can suffer from calibration errors, temporal coverage gaps, and problems with vertical resolution.

d) OH airglow imagers (Pautet et al., 2014) provide high spatio-temporal resolution 2D images of temperature perturbations derived from OH emissions near 87 km. These instruments can provide excellent wide field of view measurements over a geographic area but cannot yield vertical profiles of temperature.

e) Ground-based resonance doppler and Boltzmann lidars can derive temperatures from sodium, iron, and other meteoric metal layers in the upper mesosphere and lower thermosphere (80 - 115 km) (Chu et al., 2002). These techniques are not only useful in deriving temperature profiles but are also well situated for studies of other middle atmospheric phenomena such as gravity waves and noctilucent clouds. These lidars are restricted to measuring in the altitude band defined by the distribution of each metallic layer.

Considered together, this suite of remote sensing techniques can provide a comprehensive view of the middle atmosphere. The inclusion of Rayleigh lidar data into multi-sensor studies of the middle atmosphere provides an important local ground truthing perspective which helps to refine the global view offered by other techniques.

1.4 Outline of this Work

In this work we give a brief description of the instruments involved in the study (Sect. 2), a definition of the geographic area under consideration, and several criteria for determining coincidence between lidar and satellite measurement profiles (Sect. 3). In Sect. 4 we directly compare temperature profiles from MLS and SABER to the lidar temperatures and show a monthly median difference climatology and note several systematic differences. Section 5 details a procedure to correct the satellite temperature profiles based on the height of the stratopause in the lidar data. Finally, Sect. 6 shows an improved lidar-satellite monthly median difference climatology based on the altitude corrected satellite data.

2 Instrumentation

The Observatoire de Haute Provence (OHP) Rayleigh lidars have been in operation in southern France since 1978 and routinely produce nightly average temperature profiles of the upper stratosphere and lower mesosphere. The details of the Rayleigh lidar algorithm and the OHP lidar specifications are presented in the companion publication (Wing et al., 2018).

SABER is a broadband radiometer aboard NASA's TIMED (Thermosphere Ionosphere Mesosphere Energetics Dynamics) satellite and makes temperature measurements based on CO₂ limb radiances from 20 km to 120 km. SABER has a vertical resolution of 2 km and random temperature errors of less than 0.5 K below 55 km, 1 K at 70 km, and 5 K at 100 km (Remsberg et al., 2008). TIMED does not have a sun synchronous orbit and does not pass through our OHP comparison area at a fixed local time. This makes finding temporally coincident measurements with the lidar relatively easy. We are using version 2.0 of the published SABER temperatures. Further information for SABER/TIMED can be found in (Mertens et al., 2001).

MLS is a microwave spectrometer aboard the Aura satellite and makes temperature measurements based on emissions from O₂. Further information can be found in (Waters et al., 2006). MLS

vertical averaging kernels have a full-width-half maximum (FWHM) of 8 km at 30 km, 9 km at 45 km, and 14 km, at 80 km and a temperature resolution which goes from 1.4 K near 30 km to 3.5 K above 80 km (Schwartz et al., 2008). We are using version 4.0 of the published MLS temperatures.
165 MLS is a sun synchronous satellite which passes the equator around 1h45 UTC and is generally temporally coincident with the last hour or so of lidar measurements.

3 Comparison Parameters

Defining coincident measurements between satellites and lidars can be difficult due to temporal and spatial offsets, differences in viewing geometry, and different approaches to smoothing. Studies such
170 as García-Comas et al. (2014) have defined short time windows over a 1000 km square surrounding the observatory as sufficient for coincidence while others such as (Yue et al., 2014) have chosen to approach the problem by looking at monthly averages over a much narrower latitude band.

For this study we wanted to compare to satellite profiles geographically near the lidar to minimize latitudinal variations in the temperature and within a small time frame to minimize the contribution
175 of tides, tidal harmonics, and gravity wave effects. This desire for close spatio-temporal matching was balanced against the need for a sufficiently large number of comparisons as to produce results which are statistically significant and useful. Ultimately, we decided on a geographic window of $\pm 4^\circ$ latitude and $\pm 15^\circ$ longitude similar to the analysis done by (Dou et al., 2009). We reasoned that the UMLT (Upper Mesosphere and Lower Thermosphere) structure would vary with latitude to a
180 greater degree than with longitude and that the longitudinal separation between consecutive SABER satellite passes gives a natural bound on the longitude. The contemporaneous work by (Dawkins et al., 2018) includes a sensitivity study on the choice of longitudinal co-location limits. Their final choice for a spatial coincidence ($\pm 5^\circ$ latitude , $\pm 15^\circ$ longitude) is comparable to our study which employs ($\pm 4^\circ$ latitude , $\pm 15^\circ$ longitude). Figure 1 shows the geographic extent of our study.

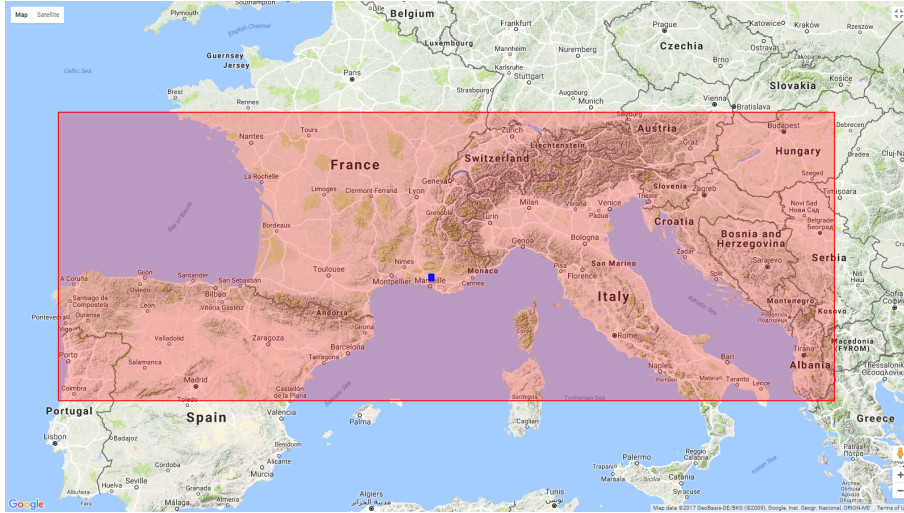


Figure 1: Area defined for coincident measurements (40° N, 9° E) to (48° N, 21° E). L'Observatoire de Haute-Provence in blue at (43.93° N, 5.71° E). (data: Google, 2017)

185 The minimum length of an OHP nightly lidar temperature measurement is four hours. We chose to use a ± 4 h window around the lidar measurement as the temporal limit for coincidence with a satellite pass. This gives us a roughly 12 h window centered around the middle of the lidar measurement. Our choice was influenced by a desire to minimize the effect of the 12 h tidal harmonic. Previous work comparing between satellites have been able to take advantage of daytime satellite overpasses and chose to work within a ± 2 h window (Hoppel et al., 2008). (French and Mulligan, 2010) conducted a comparison between an OH spectrometer (in conjunction with a sodium lidar) and SABER at ± 15 min and ± 8 h and found no significant difference. However, it must be noted that this study was conducted at a latitude of 69° S and the comparison may not hold in the mid-latitudes.

4 Temperature comparisons without considering vertical offset

195 Here we demonstrate the directly-calculated temperature biases between OHP and both SABER and MLS which are present before we carry out the adjustment for satellite altitude offsets which are discussed in Sect. 5. An example of all three temperature profiles for the night of the 25th of July 2012 is shown in Fig. 2. In this comparison the lidar profile was produced over 4 hours and has a vertical resolution of 150 m from 30 km to above 90 km. The large temperature uncertainty above 200 70 km is a result of the fine vertical resolution required to capture the mesospheric inversion layer present near 77 km.

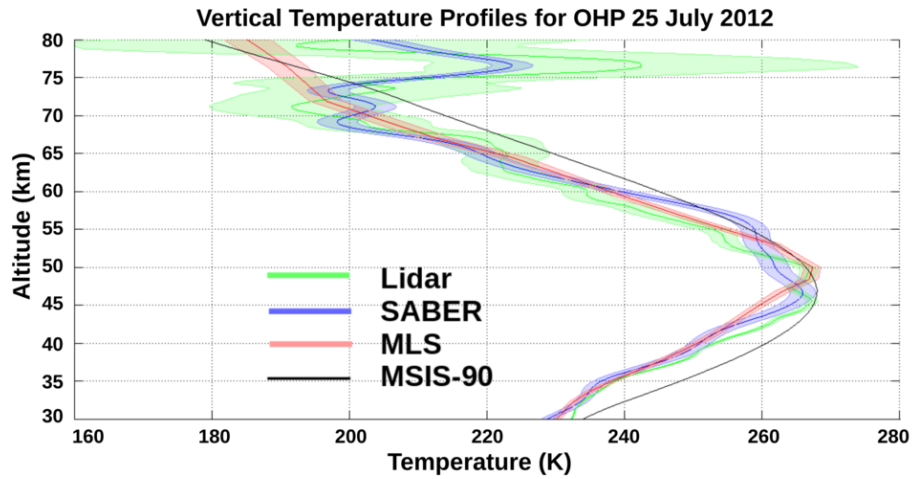


Figure 2: Example co-located temperature profiles from the OHP lidar (green), SABER (blue), MLS (red), and MSIS (black).

4.1 Comparison OHP Lidar and SABER

From 2002 to 2018 there were 1100 coincident measurements of sufficient quality between OHP lidars and SABER. Figure 3 (upper panel) shows the monthly median temperature differences between the lidar and SABER while Fig. 3 (lower panel) shows the mean seasonal temperature bias with altitude.

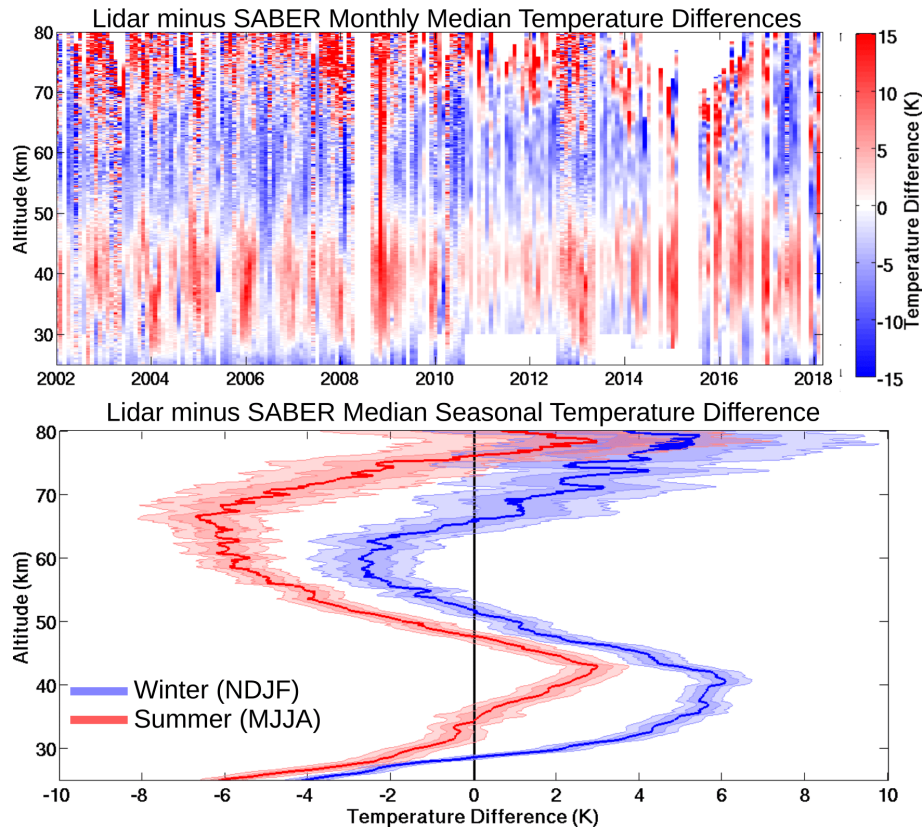


Figure 3: Sixteen year systematic comparison of OHP lidars and SABER temperatures. The monthly median temperature differences between the lidar and SABER are shown in the upper panel. Red indicates that the lidar is warmer than SABER and blue that the lidar is colder. There are 1100 nights of coincident measurements in the colour plot. The lower panel is a seasonal ensemble of lidar minus SABER temperature differences. The summer (May, June, July, August) ensemble in red includes 306 nights of coincident measurements and the winter (November, December, January, February) ensemble in blue includes 397 nights of coincident measurements. Shaded errors represent 1 and 2 standard deviations.

Figure 3 upper panel contains the monthly median temperature differences between an OHP lidar temperature profile and a SABER temperature profile. After 2010 there are several time periods where the Lidar Température et Aérosol (LTA) was not in routine operation or was in the process of being upgraded. To fill in these data gaps we have used temperature profiles derived from the ozone Differential Absorption Lidar (DIAL), also referred to as Lidar Ozone Stratosphère (LiO₃S), which is described and validated for temperature in (Wing et al., 2018). Given that the main scientific interest of LiO₃S is stratospheric ozone, the noise floor of the raw lidar signal occurs a lower altitude than for LTA for similar vertical integration. To produce temperature profiles which extend into the

215 mesosphere we use a coarser vertical resolution, a minimum altitude of 30 km, and often stop the
temperature profile below 80 km if the temperature error becomes excessive.

The upper panel shows a relative warm bias for the lidars with respect to SABER above 70 km.
Discrepancies in this region are likely due to lidar initialization errors and background uncertainty
which we have attempted to minimize in the companion publication (Wing et al., 2018). There is also
220 an evident seasonal relative warm bias in the winter stratosphere between 30 km and 50 km - a region
where lidar uncertainties in both altitude and temperature are well described (Leblanc et al., 2016)
(Leblanc et al., 2016). The lower panel shows a very distinctive ‘S’ shape to the bias in both the
winter and summer ensembles which is indicative of a vertical offset between the lidar and satellite
measurements. The basic ‘S’ shape bias was identified in studies of synthetic lidar data as being
225 due to vertical offsets between lidar instruments (Leblanc et al., 1998). Unfortunately, this offset is
neither constant from night to night, nor constant with altitude as evidenced by the elongated and
distorted nature of the ‘S’ shape.

If we bin all the temperature differences by month we can clearly see that there is a winter strato-
spheric warm bias below 45 km and a pronounced summer cold bias in the mesosphere between 50
230 and 70 km, as shown in Fig. 4.

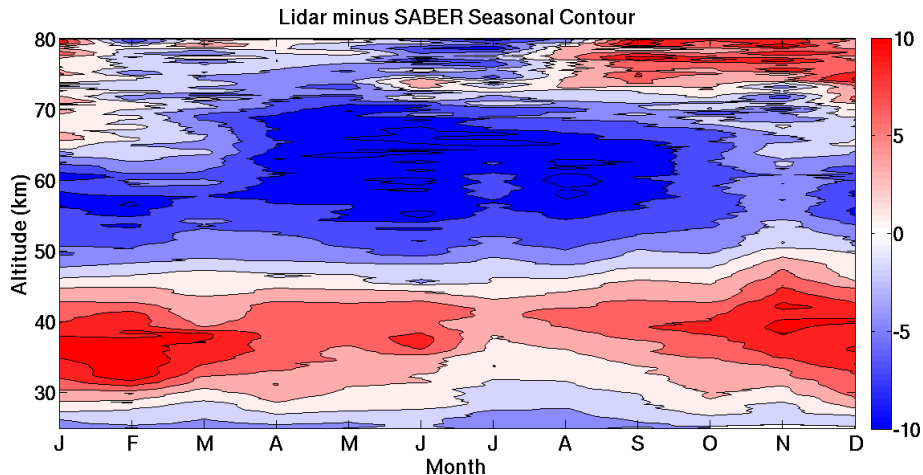


Figure 4: Monthly median temperature difference between lidar and SABER temperature measurements. Red indicates regions where the lidar measures warmer temperatures than SABER and blue regions where the lidar measures colder temperatures than SABER.

4.2 Comparison OHP lidar and MLS

From 2004 to 2018 there were 1741 coincident measurements of sufficient quality between OHP lidars and MLS. Figure 5 (upper panel) shows the monthly median temperature differences between the lidar and MLS while Fig. 5 (lower panel) shows the mean seasonal temperature bias with altitude.

235 As was the case with the lidar-SABER comparison, in the upper panel we see a lidar warm bias
 above 70 km and a strong winter stratospheric warm bias near 45 km. In this comparison the strato-
 spheric warm bias appears to have a downward phase migration as the winter progresses. In the
 corresponding lower panel we see very pronounced summer time systematic differences which al-
 ternate from warm to cold throughout the stratosphere and mesosphere. The winter ensemble shows
 240 a very large lidar warm bias near the stratopause.

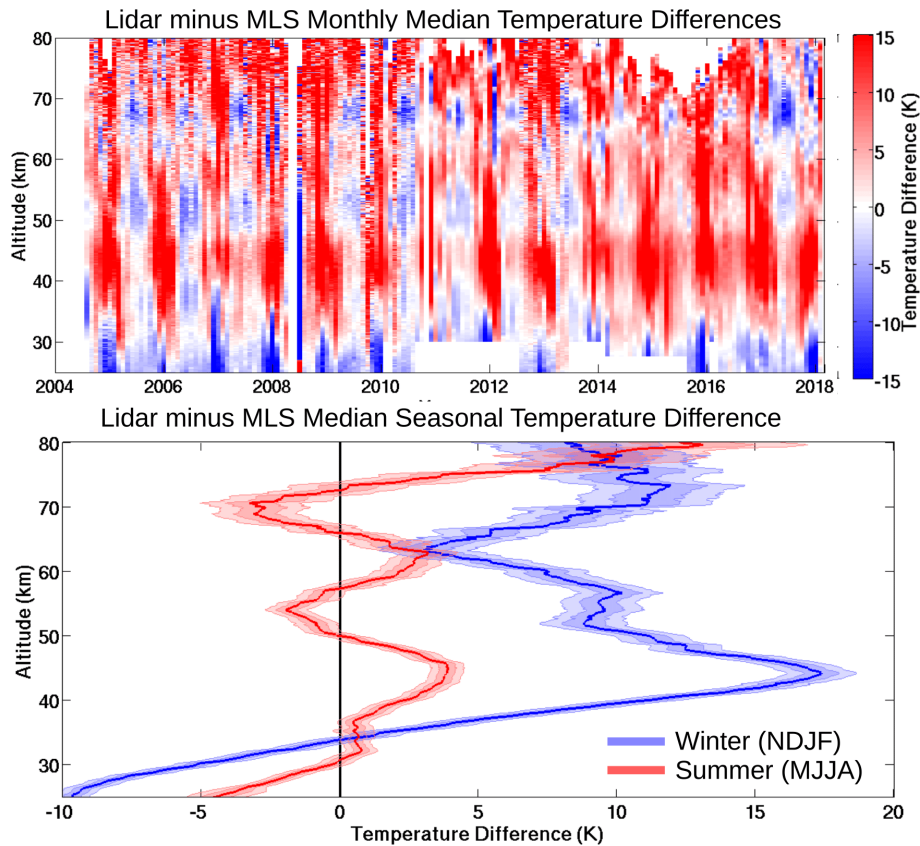


Figure 5: Fourteen year systematic comparison of OHP lidar and MLS temperatures. The monthly median temperature differences between the lidars and MLS are shown in the upper panel. There are 1741 nights of coincident measurements. The lower panel is a seasonal ensemble of lidar minus MLS temperature differences. The summer (May, June, July, August) ensemble in red includes 554 nights of coincident measurements and the winter (November, December, January, February) ensemble in blue includes 653 nights of coincident measurements. Shaded errors represent 1 and 2 standard deviations.

Following the same procedure of binning lidar-MLS temperature differences by month we see a very pronounced downward phase progression of the winter stratospheric warm bias from 45 km in January descending down to 40 km in February and March. Additionally, there is an evident layered

cold bias in the summer stratosphere and mesosphere. The three layers appear near 37 km, 53 km, and 68 km in Fig. 6.

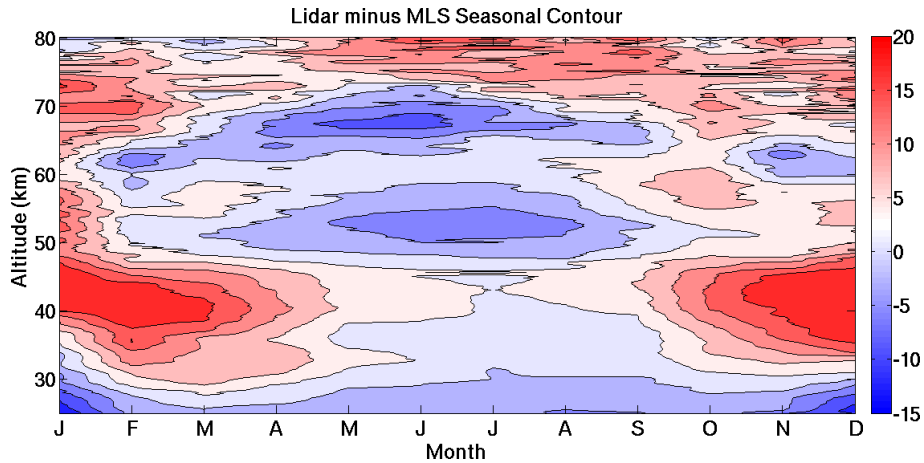


Figure 6: Monthly median temperature difference between lidar and MLS temperature measurements. Red indicates regions where the lidar measures warmer temperatures than MLS and blue regions where the lidar measures colder temperatures than MLS.

5 Minimizing Temperature Difference Between Lidar and Satellites with a Vertical Offset

We investigated a possible vertical offset between the lidar and satellite measurements to determine whether this could be contributing to the temperature biases seen in Sect. 4.

5.1 Method to determine the vertical offset between measurements

250 To match the two temperature profiles exactly in amplitude and altitude requires a unique altitude dependent correction factor for each comparison. However, we can make a rough estimate of the average vertical offset between the two measurements by focusing on the region of the stratopause which generally has a defined altitude and a clear structure. We used a simple least squares method to best estimate the vertical offset that would minimize the temperature differences between the lidar
 255 measurement and the satellite measurement. Two examples of this offset calculation for SABER are shown in Fig. 7 and two examples for MLS are shown in Fig. 8. The examples in these figures show nights where the lidar and satellite temperatures are in good agreement or can be brought into good agreement by applying a small vertical displacement. However, it is important to note that there are examples of lidar-satellite temperature measurements which cannot be brought into good agreement
 260 with small vertical displacements. Two such examples can be found in Fig. 9. These examples of poor agreement are almost exclusively found in winter on nights where the stratopause is greatly disturbed.

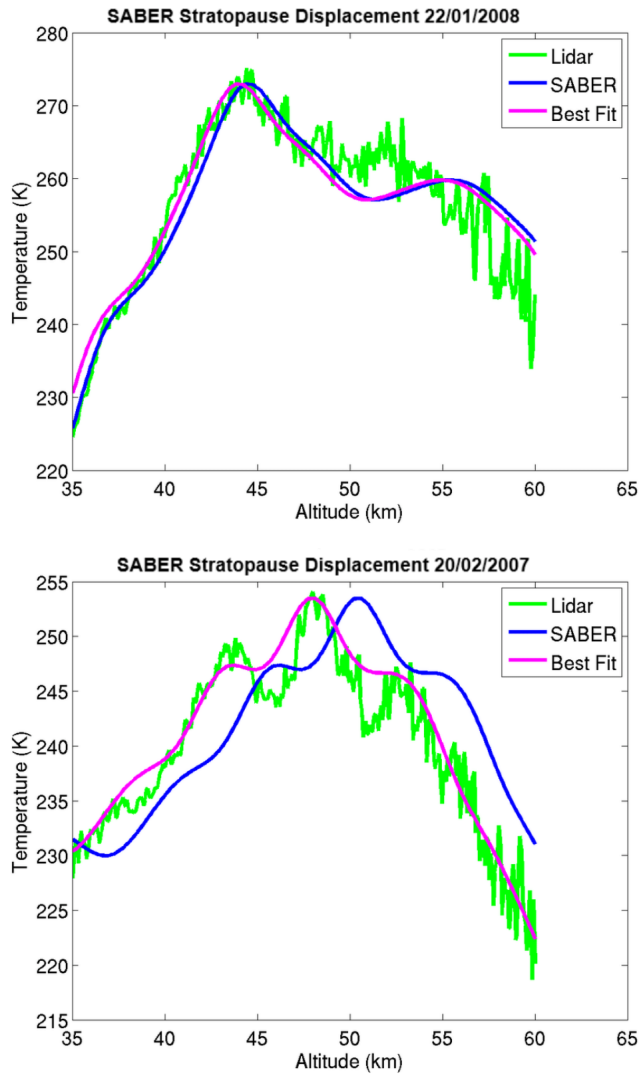


Figure 7: The upper panel shows a case where the lidar and SABER were well aligned in altitude. The lower panel shows a case where a vertical displacement of the SABER profile ameliorated the agreement with the lidar measurement.

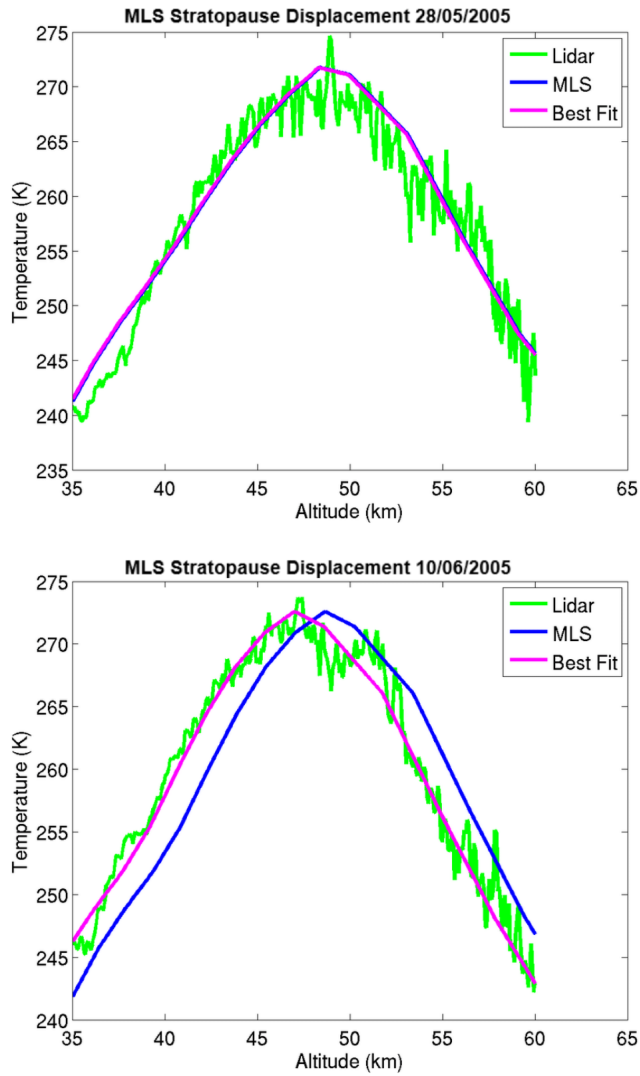


Figure 8: The upper panel shows a case where the lidar and MLS were well aligned in altitude. The lower panel shows a case where a vertical displacement of the MLS profile ameliorated the agreement with the lidar measurement.

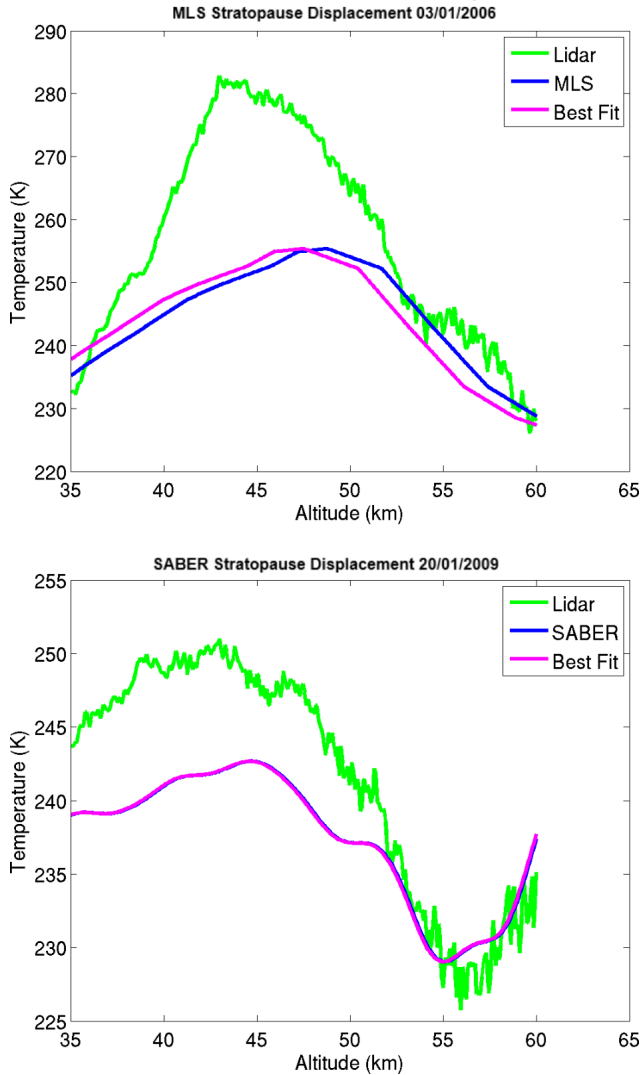


Figure 9: Two examples of poor matches between lidar and satellite temperature profiles (MLS upper panel, SABER lower panel). These mismatches mainly occur between late November and early April on nights where the stratosphere was disturbed and experiencing a warming.

5.2 Trends in Vertical Offset between Lidar and Satellites

We calculated an offset for every coincident measurement between the lidars and SABER and the lidars and MLS. The monthly average of this altitude offset value is represented in Fig. 10 as a green line for years where the comparisons were primarily between LTA and the satellites and as a blue line for years where LiO_3S temperatures were used. The green and blue shaded regions are the respective standard deviations. Given the reduced vertical resolution of the temperature profiles from LiO_3S , the least-squares minimized correction for stratopause height is less sensitive to small and medium scale fluctuations in the temperature profiles such as the triple peak structure seen in the lower

panel of Fig. 7. As a result, comparisons between LiO₃S and both satellites (blue curve in Fig.10) tend toward the mean altitude displacement. This effect is more pronounced when comparing with SABER, which has a finer vertical resolution, than when comparing with MLS which has a coarser vertical resolution. There is a clear, but imperfect, seasonality to these altitude displacements.

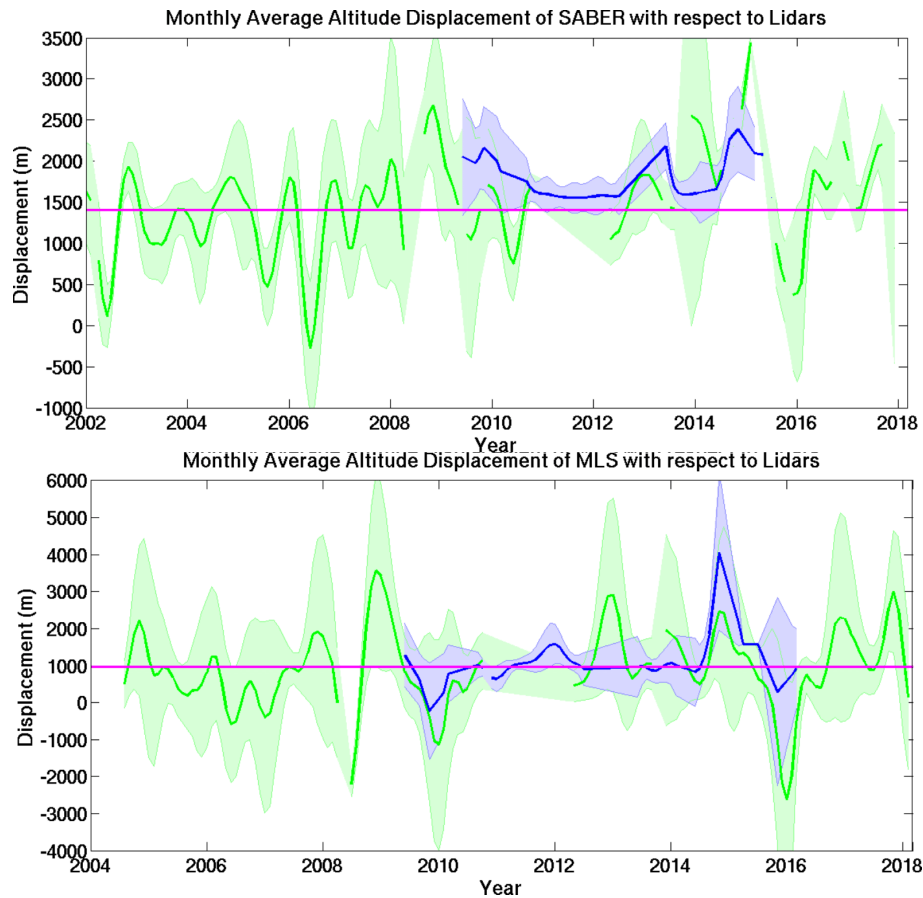


Figure 10: The upper panel features the monthly average displacement of SABER measurements with respect to the OHP lidars (green for LTA and blue for LiO₃S). The standard deviation is given as the shaded area. The mean offset (magenta) is 1446 m with a standard error of 49 m. The lower panel shows the same analysis with the monthly average MLS displacement. The mean value is 911 m with a standard error of 90 m.

275 Superimposing the traces shown in Fig. 10 onto the colour plots in Fig. 3 and Fig. 5 shows a clear correlation between lidar-satellite temperature anomalies and mean monthly altitude displacement between the lidar and satellite temperature profiles, as shown in Fig. 11.

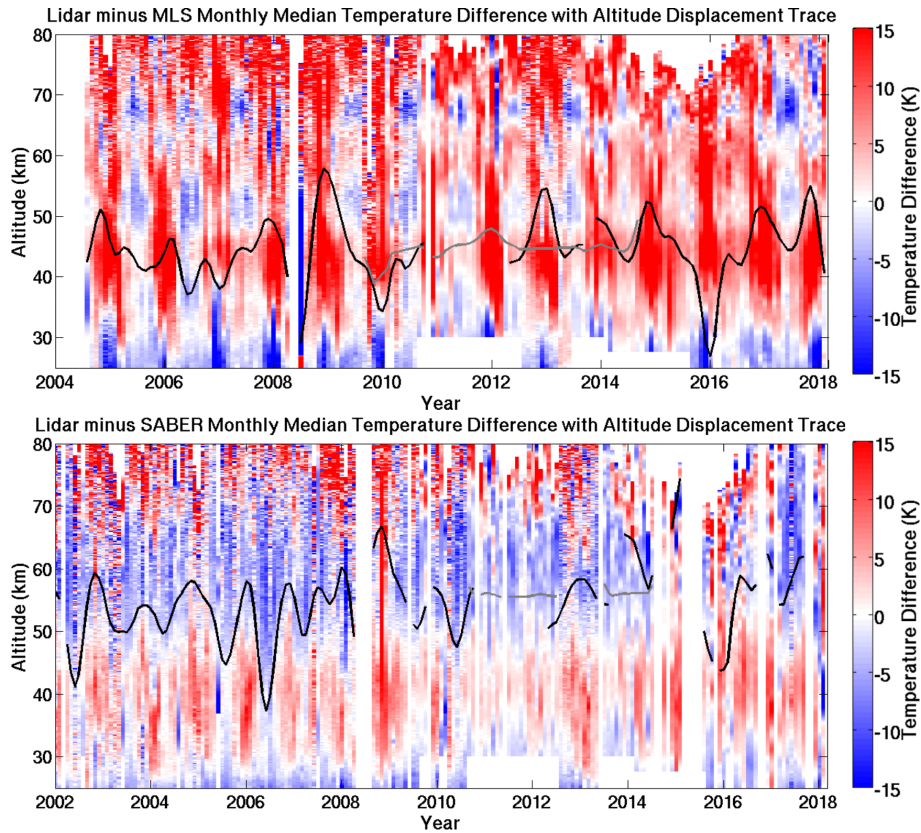


Figure 11: The upper panel features the monthly median temperature differences between the lidar and MLS seen in 5 with the estimated vertical displacement of the stratopause height overplotted. The lower panel features the monthly median temperature differences between the lidar and SABER seen in 3 with the estimated vertical displacement of the stratopause height overplotted. The black line represents comparisons between LTA and the satellite and the grey line represents comparisons between LiO₃S and the satellite.

6 Recalculated Lidar-Satellite Temperature Differences

We have attempted to make a more accurate comparison of the lidar and satellite temperatures by using the stratopause height as a common altitude reference. We re-calculated the lidar-satellite temperature differences shown in Fig. 4 and Fig. 6 after displacing the satellite measurement by a scalar value. Each satellite measurement was shifted vertically according to the lidar derived stratospheric displacements shown in Fig. 10.

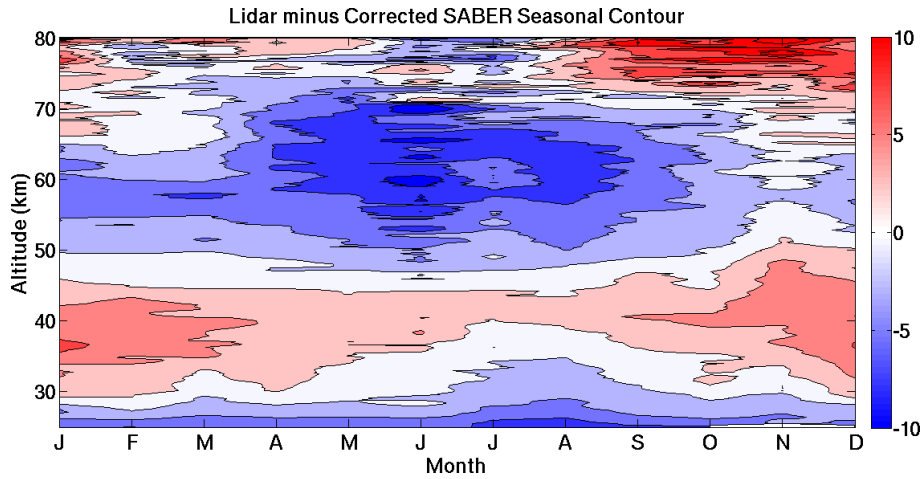


Figure 12: Corrected seasonal temperature differences between the lidar and the vertically displaced SABER temperatures. The magnitude of the temperature differences is reduced in both the stratosphere and mesosphere over the majority of the altitude range when compared to a similar uncorrected temperature difference contour seen in Fig. 4.

In Fig. 12 we see that by displacing the SABER temperature profiles so that the stratopause height
 285 is the same in both the lidar and satellite measurements we have reduced the maximum winter time
 stratospheric warm bias from approximately 8 K to 4 K. The summer time mesospheric cold bias
 of -10 K has likewise been reduced by between 4 and 6 K depending on altitude and season. The
 remaining bias in both the stratosphere and mesosphere cannot be further minimized by a simple
 vertical shift. The altitude dependent correction which would be required to correct the temperature
 290 lapse rate is beyond the scope of this work.

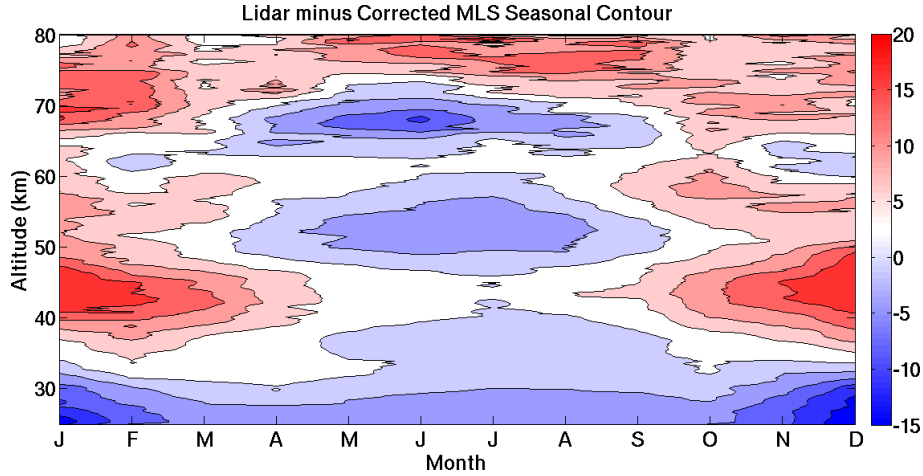


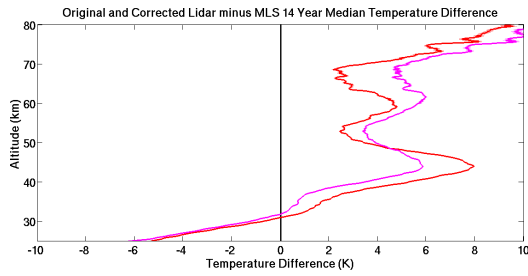
Figure 13: Corrected seasonal temperature differences between the lidar and the vertically displaced MLS temperatures. The structured nature of the temperature bias seen in Fig. 6 remains unchanged by the vertical correction.

In Fig. 13 we see that displacing the MLS temperature profiles was less successful than in the case of the SABER measurements. We have reduced the magnitude of beginning and end of winter time stratospheric warm bias by up to 5 K during the months of March, April, October, and November but the correction does not completely eliminate the issue. As well we have an improvement of 5 K
 295 in the biased layer at 65 km. However, the horizontal layering inherent in the MLS temperature data makes determining a scalar correction even more challenging than in the case of SABER.

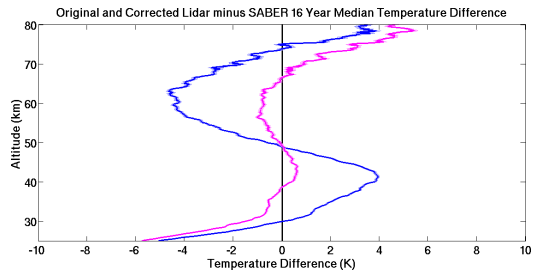
We have replotted the seasonal ensemble temperature difference curves shown in the lower panel of Fig. 3 (lidar-SABER) and Fig. 5 (lidar-MLS) alongside the ensemble temperature differences after we applied the correction for stratopause height. Figure 14a shows the ensemble temperature
 300 difference for all 1741 lidar-MLS temperature comparisons before correction (red) and after correction (magenta). The prominent warm bias near 45 km has been reduced from 8 K to 6 K but the cold biases at 53 km, and 68 km are made worse by the correction. To understand this result we can look at the seasonal dependence of the applied correction. Figure 14c is the summer ensemble temperature difference (MJJA) consisting of 554 lidar-MLS temperature comparisons before correction
 305 (red) and after correction (magenta). There is marginal improvement after correction below 55 km but the change is not significant at 2σ and the structure of the temperature bias remains unchanged. Figure 14e is the winter ensemble temperature difference (NDJF) consisting of 653 lidar-MLS temperature comparisons before correction (blue) and after correction (magenta). There is significant improvement of 4 K in the large cold bias at 45 km. The corrected lidar-MLS comparison is also
 310 significantly worse near the cold bias at 63 km.

Figure 14b shows the ensemble temperature difference for all 1100 lidar-SABER temperature comparisons before correction (blue) and after correction (magenta). the stratopause height correc-

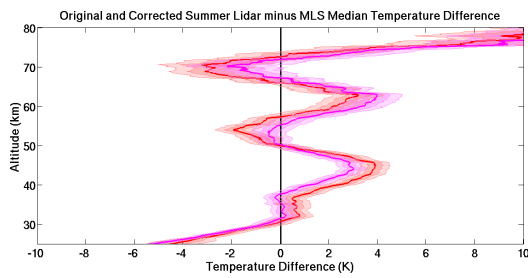
tion has reduced the stratospheric warm bias from 4 K to less than 1 K and has reduced the meso-
spheric cold bias from -4 K to -1 K. The warm bias above 70 km has been slightly increased. Figure
315 14d is the summer ensemble temperature difference (MJJJ) consisting of 306 lidar-SABER temper-
ature comparisons before correction (red) and after correction (magenta). There is a significant 3 K
reduction in the warm bias at 45 km and a significant reduction in the mesospheric cold bias from
-6 K to -3 K. Figure 14f is the winter ensemble temperature difference (NDJF) consisting of 397
lidar-SABER temperature comparisons before correction (blue) and after correction (magenta). By
320 applying the altitude correction we have eliminated the 'S' shape in the temperature difference curve
between 30 and 60 km. There is a significant 1 K constant warm bias that remains after correction.
Above 70 km there is no statistically significant change.



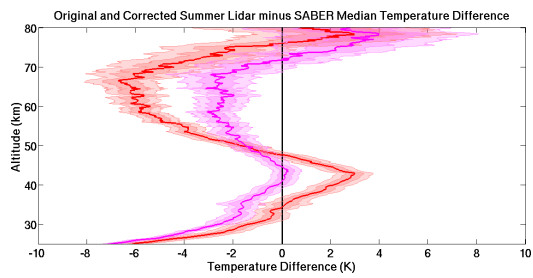
(a) Median temperature difference for 1741 lidar minus MLS temperature profiles from 2004 to 2018. Red is the original ensemble and magenta is the ensemble after correction.



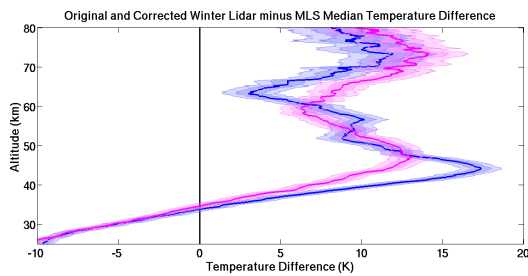
(b) Median temperature difference for 1100 lidar minus SABER temperature profiles from 2002 to 2018. Blue is the original ensemble and magenta is the ensemble after correction.



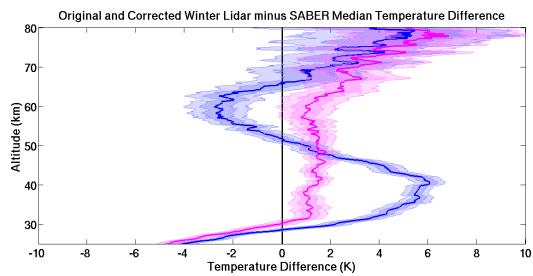
(c) Median summer (MJJA) temperature difference for 554 lidar minus MLS temperature profiles from 2004 to 2018. Red is the original ensemble and magenta is the ensemble after correction.



(d) Median summer (MJJA) temperature difference for 306 lidar minus SABER temperature profiles from 2002 to 2018. Red is the original ensemble and magenta is the ensemble after correction.



(e) Median winter (NDJF) temperature difference for 653 lidar minus MLS temperature profiles from 2004 to 2018. Blue is the original ensemble and magenta is the ensemble after correction.



(f) Median winter (NDJF) temperature difference for 397 lidar minus SABER temperature profiles from 2002 to 2018. Blue is the original ensemble and magenta is the ensemble after correction.

Figure 14: Ensemble for lidar minus MLS temperature differences (left) and lidar minus SABER (right). Ensembles for all profiles are on the top row, summer (MJJA) profiles in the middle row, and winter (NDJF) in the bottom row.

7 Discussion

7.1 The need for vertical altitude correction of satellite data

325 Improved observations of stratospheric and mesospheric temperature profiles and dynamical phe-
nomena are required to advance our understanding of the middle atmosphere. The process of ground
to satellite measurement comparison and validation is a vital ongoing scientific activity. By compar-
ing long term, stable, continuous, high quality temperature measurements, such as those made by the
lidars at OHP, to other datasets we can help to identify potential issues with calibration or retrieval
330 algorithms.

We have presented individual cases in Fig. 7 and Fig. 8 where both MLS and SABER tempera-
ture profiles benefited from a slight vertical displacement based on lidar derived stratopause height.
While this scalar adjustment does not correct for non-linear distortions in the altitude vector it can
significantly reduce the magnitude of the temperature bias in the stratosphere and lower mesosphere
335 as seen in Fig. 14a and Fig. 14b. This technique does not seem to work well when the stratopause
is highly disturbed as can be seen in the two winter time examples in Fig. 9. The implications of
satellite underestimation of sudden stratospheric warming events is of particular concern to reanal-
ysis projects attempting to model middle atmosphere dynamics. However, by using lidar data to
supplement the satellite record these fast dynamical processes can be better resolved.

340 An additional point about vertical resolutions should be made before further interpreting the re-
sults of our lidar-satellite temperature comparison. As was noted in sect. 2 both MLS and SABER
measure radiances on a pressure grid with reported vertical averaging kernels whereas the lidar mea-
sures temperature on a fixed geometric altitude grid. SABER has a relatively small and uniform
vertical resolution with a FWHM of 2 km and MLS has a somewhat lower vertical resolution in the
345 middle atmosphere, which increases with height, reaching a FWHM of 15 km at the top of our com-
parison region at 80 km. To make a fair comparison we have reduced the lidar vertical resolution to
accommodate the satellites. There are considerations to keep in mind when comparing the results of
the lidar-SABER and lidar-MLS temperature biases. First is the effect that vertical resolution has on
the temperature difference profile. SABER has a smaller FWHM and is therefore much more likely
350 to reproduce the small scale variations seen in the lidar data. This means that sharp features like the
stratopause can easily be used as a tool for detecting possible bias. In contrast, MLS has a much
wider FWHM which means that we expect much less vertical fidelity in the lidar comparison. The
lower vertical resolution should act to smooth out the temperature peaks and valleys in a way that
may not correspond to the higher resolution ground based measurements.

355 7.2 Temperature biases between OHP lidar and SABER

In the companion publication (Wing et al., 2018) we attempted to reduce the magnitude of the
initialization induced lidar warm bias which is often reported above 70 km. We have reduced the

bias by up to 5 K near 85 km and nearly 20 K at 90 km. There still remains some residual systematic warm bias between the lidar satellite comparisons in this publication.

360 The average 9.9 ± 9.7 K bias at 80 km reported by (Dawkins et al., 2018) using 9 different metal layer resonance lidars compares favorably to our ensemble bias of 5 K at 80 km Fig. 14b. Given that the resonance lidars do not initialize their temperatures using the same inversion algorithm as the Rayleigh lidars, and that the resonance lidars have a minimum uncertainty near 85 km, perhaps our Rayleigh temperatures are not as influenced by a priori as we thought. Further work needs to be
365 done on the topic of initialization related bias to fully address the effects of noise and a priori choice on high altitude Rayleigh lidar retrievals. However, we are encouraged by our results and cannot discount the possibility that some of the remaining temperature difference is due to errors or bias in the satellite altitudes.

When considering the residual temperature differences between the OHP lidars and SABER after
370 the altitude correction based on lidar derived stratopause height we can see that much of the seasonally varying bias in the stratosphere and mesosphere has been reduced. We are still left with a general summer time cold bias over most of the atmospheric column, except near 45 km, which now achieves a maximum of -4 K in the June mesosphere. We cannot explain this bias from the perspective of the lidar data as nothing in our range resolution changes, our data acquisition cadence and
375 measurement duration are very similar (Wing et al., 2018), and we are well into the linear region of lidar count rates and are not influenced by our a priori or saturated count rates. It is possible that there could be a tidal contribution as summer time lidar measurements start a bit later than winter time measurements due to a shorter astronomical night. However, given that our criteria for coincidence were chosen to minimize the effects of the first few tidal harmonics this seems unlikely. It is also
380 possible that there is a seasonally dependent bias in the a priori used in the satellite retrieval of the geopotential height which could influence the satellite altitude vector.

The cold bias seen below 30 km is most likely due to possible contamination in the lidar data from aerosols and saturation in the low gain Rayleigh channel. Current OHP lidar measurements use Raman scatter data to correct for these effects and produce temperature profiles down to 5 km.
385 However, this Raman data is not available for the entire 2002 to 2018 analysis period so we have opted not to include it in this work.

7.3 Temperature biases between OHP lidar and MLS

As with the comparison between the lidar and SABER, the lidar and MLS comparison has a pronounced warm bias above 70 km which is in keeping with previous studies. However, the magnitude
390 and extent of this warm bias in MLS is much more pronounced than in the SABER comparison plot. Much of this difference is due to the reduced vertical resolution of MLS at these high altitudes. This holds true particularly when comparing lower vertical resolution lidar data to MLS.

The lidar MLS comparison has a winter time stratospheric warm bias which is not much reduced by simply shifting the location of the MLS stratopause (Fig. 14e). We have reduced the magnitude of the difference by 4 K but the stratopause altitude correction was markedly less successful than in the case with SABER. It is almost universally the case that sudden stratospheric warmings seen by the lidar are missed or smoothed over in the corresponding MLS measurement. Figure 9 (upper panel) is very much a typical comparison for periods when the stratosphere is highly disturbed. There is a limit to how much can be done to improve the lidar-MLS comparison using a simple scalar correction.

The vertical structure which dominates much of the middle portion of the lidar MLS comparison is also difficult to account for. The structure is particularly evident in Fig. 14c and is nearly insensitive to our applied altitude correction. There is nothing in the lidar technique that could explain this pattern. A similar horizontal banding pattern is seen in the comparison of MLS to The European Center for Medium-range Weather Forecasts (ECMWF) assimilation in the MLS geopotential validation paper (Schwartz et al., 2008). The effect is most likely an artefact introduced in some stage of the satellite retrieval. Studies like ours provide a perfect opportunity to incorporate lidar information into the satellite retrieval and improve the satellite data products. Given the confidence we have in the fixed width and amplitude of the vertical kernels in the lidar measurement, a lidar altitude and temperature vector could be used to recalculate the MLS geopotential and temperature profiles to help identify the source of this artefact.

It is also important to acknowledge that simply correcting for stratopause height offset was counter productive for our lidar-MLS comparisons above 50 km as seen in Fig. 14a. It is likely that any potential lidar-derived correction for MLS will be more complex than a simple scalar offset. Such a correction may even have different functional forms in the stratosphere and mesosphere.

7.4 Comparison with previous work

We can compare our results to a few of the studies involving Rayleigh lidar cited in the introduction however, it is important to note a few caveats. The methodologies of the different studies vary significantly and a direct comparison between our work and previous studies is fraught with confounding variables, differences in sampling size, and statistics. As a brief reminder, our work was done in a 30 by 8 degree geographic box centred on the OHP and had a temporal coincidence window of 12 hours. We then made nightly average temperature differences between the lidar and satellites and presented the monthly medians of those temperature differences over span of each satellite (2002-present for SABER and 2004-present for MLS).

The two studies by Sivakumar (Siva Kumar et al., 2003), (Sivakumar et al., 2011) made use of monthly averaged lidar and SABER temperatures and found semi annual temperature anomalies of 3-5 K in the stratopause region during February-March and September-October which was attributed to averaging and possibly the Annual Oscillation. We have shown a similar temperature difference in the stratopause of 4 K in the summer before altitude corrections, reduced to zero bias after altitude

correction, and 6 K in the winter before altitude corrections, reduced to 1 K after altitude correction.

430 We have correlated this temperature bias directly to a vertical displacement of the satellite altitude with respect to the lidar altitude and not with the Annual Oscillation. Further work must be done to explore the possibility of North Atlantic Oscillation/Annual Oscillation effects but a quick correlation of relative vertical displacement seen in Fig. 10 and a monthly average AO phase shows an R squared value of only 0.04 for SABER and 0.03 for MLS. There are isolated periods of up to a year
435 where it seems like the correlations are significant however, it is clear that over a period of nearly a decade the AO phase and winter time stratospheric temperature anomaly are not correlated.

The study by (Yue et al., 2014) compared 120 nights of lidar temperatures to SABER monthly average temperatures and found winter time temperature anomalies in the stratopause region of 5 K. The stratospheric warm bias was attributed to tides, however, this explanation cannot explain the
440 seasonal nature of this bias found in this work nor explain why a simple vertical displacement of the satellite stratopause height offers a suitable correction. Subsequent to this work (Hauchecorne et al., 2018) have published a temperature dataset derived from GOMOS stellar occultation measurements which were validated using Rayleigh lidar. In this article, the tidal contribution to the lidar-satellite temperature bias in the stratosphere is estimated to be less than 2 K based on tidal characteristics
445 extracted from the Global Scale Waves Model for tides.

The same 2-5 K stratopause temperature bias was found by (Dou et al., 2009). This study used 2332 nights of lidar data from 6 different NDACC lidars and compared with the zonal mean temperatures from SABER. The bias was attributed to possible tidal aliasing or aerosol contamination. In part 1 of this article we note that contamination by aerosols is not significant above 30 or 35 km and
450 that aerosols cannot be responsible for lidar temperature bias in the stratopause. As was stated in the previous paragraph, (Hauchecorne et al., 2018) estimate an upper limit on the effect of tidal aliasing for a small geographic area of less than 2 K. It is possible that tides could play a larger role when comparing measurements from a localised lidar ground site to a zonal average temperature from a satellite. The altitude corrections shown in the present manuscript account for all 4 K of temperature
455 bias in summer, and 5 of 6 K of bias during winter. This type of correction may account fully for the stratopause temperature bias reported by (Dou et al., 2009).

In summary, previous studies have shown a consistent systematic temperature bias of 2 to 5 K between different independent lidars and SABER near the stratopause. Tides, aerosols, planetary oscillations, and satellite calibration errors were all given as possible sources of error when accounting
460 for this discrepancy. Our study has shown that the temperature bias has a clear seasonality, with the largest temperature differences occurring in the winter months. We have also shown that a simple vertical correction of the satellite temperatures based on the height of the stratopause, as measured by the lidar, significantly reduces the bias.

8 Conclusions

465 We can draw the following conclusions from the comparison of the lidar and satellite temperature measurements.

1) We have found the same systematic 5-15 K warm bias in the lidar-satellite comparisons above 70 km found in studies like (García-Comas et al., 2014), (Taori et al., 2011), (Taori et al., 2012b), (Taori et al., 2012a), (Dou et al., 2009), (Remsberg et al., 2008), (Yue et al., 2014), (Dawkins et al., 470 2018), and (Sivakumar et al., 2011). We have attempted to carefully account for the the background-induced warm bias in high altitude Rayleigh lidar temperatures. We believe that the algorithm set out in the companion publication (Wing et al., 2018) is robust and accounts for many of the uncertainties in the lidar initialization process. However, we are as yet unable to determine to what extent the a priori estimate warms the lidar temperature retrieval at these heights.

475 2) We have seen a layered summer stratosphere-mesosphere cold bias in lidar-MLS seasonal temperature comparisons with peak differences at 37 km, 50 km, and 65 km. There is nothing in the lidar data or retrieval algorithm which could account for this structure. The results of this study will be useful for any future satellite validation studies in the style of (Schwartz et al., 2008) where lidar data could be used as a reference dataset. In particular, lidar - satellite bias study results are useful 480 for the ongoing NASA project "The Mesospheric and Upper Stratospheric Temperature and Related Datasets" (MUSTARD) which seeks to merge historic and ongoing satellite datasets.

3) The persistent summertime cold bias between the lidar and SABER results from a disagreement in the thermal lapse rate above and below the stratopause which is independent of the scalar stratopause height offset. Given that lapse rate is a fundamental geophysical parameter further work 485 must be done to explore possible errors in vertical resolution and altitude definition.

4) The periods of greatest lidar-satellite temperature disagreement are found during times when the middle atmosphere is highly disturbed. In particular, the amplitude of stratospheric warming events can be underestimated and features like double stratopauses can be missed in the satellite measurements.

490 We have shown that ground based lidars can provide reliable and consistent temperature measurements over decades. This kind of high vertical resolution temperature database is useful both as a validation source for other instruments as well as for fundamental geophysical research.

Acknowledgements. The data used in this publication were obtained as part of the Network for the Detection of Atmospheric Composition Change (NDACC) and are publicly available (see <http://www.ndacc.org>, <http://cds-espri.ipsl.fr/NDACC>) as well as from the SABER (see <ftp://saber.gats-inc.com>) and MLS (see <https://mls.jpl.nasa.gov>) data centres for the public access via their websites. This work is supported by the project Atmospheric dynamics Research InfraStructure Project (ARISE 2) funded by funded by the European Union's Horizon 2020 research and innovation programme under grant agreement No. 653980 French NDACC activities are supported by Institut National des Sciences de l'Univers/Centre National de la Recherche Scientifique (INSU/CNRS),

500 Université de Versailles Saint-Quentin-en-Yvelines (UVSQ), and Centre National d'Études Spatiales (CNES).
The authors would also like to thank the technicians at La Station Géophysique Gérard Mégie at OHP .

References

- Chu, X., Pan, W., C Papen, G., Gardner, C., and A Gelbwachs, J.: Fe Boltzmann Temperature Lidar: Design, Error Analysis, and Initial Results at the North and South Poles, *Applied optics*, 41, 4400–10, 2002.
- 505 Council, N. R.: *Earth Science and Applications from Space: National Imperatives for the Next Decade and Beyond*, The National Academies Press, Washington, DC, doi:10.17226/11820, <https://www.nap.edu/catalog/11820/earth-science-and-applications-from-space-national-imperatives-for-the>, 2007.
- data: Google, M.: Observatoire de Haute Provence (CNRS) Kernel Description, [https://www.google.fr/maps/place/Observatoire+de+Haute+Provence+\(CNRS\)/@43.9236737,5.7183398](https://www.google.fr/maps/place/Observatoire+de+Haute+Provence+(CNRS)/@43.9236737,5.7183398), 2017.
- 510 Dawkins, E. C. M., Feofilov, A., Rezac, L., Kutepov, A. A., Janches, D., Höffner, J., Chu, X., Lu, X., Mlynczak, M. G., and Russell, J.: Validation of SABER v2.0 Operational Temperature Data With Ground-Based Lidars in the Mesosphere-Lower Thermosphere Region (75–105km), *Journal of Geophysical Research: Atmospheres*, 0, doi:10.1029/2018JD028742, 2018.
- Dou, X., Li, T., Xu, J., Liu, H.-L., Xue, X., Wang, S., Leblanc, T., McDermid, I. S., Hauchecorne, A., Keckhut, P., Bencherif, H., Heinselmann, C., Steinbrecht, W., Mlynczak, M. G., and Russell, J. M.: Seasonal oscillations of middle atmosphere temperature observed by Rayleigh lidars and their comparisons with TIMED/SABER observations, *Journal of Geophysical Research: Atmospheres*, 114, doi:10.1029/2008JD011654, <http://dx.doi.org/10.1029/2008JD011654>, d20103, 2009.
- 515 French, W. J. R. and Mulligan, F. J.: Stability of temperatures from TIMED/SABER v1.07 (2002–2009) and Aura/MLS v2.2 (2004–2009) compared with OH(6–2) temperatures observed at Davis Station, Antarctica, *Atmospheric Chemistry and Physics*, 10, 11 439–11 446, doi:10.5194/acp-10-11439-2010, <https://www.atmos-chem-phys.net/10/11439/2010/>, 2010.
- García-Comas, M., Funke, B., Gardini, A., López-Puertas, M., Jurado-Navarro, A., von Clarmann, T., Stiller, G., Kiefer, M., Boone, C. D., Leblanc, T., Marshall, B. T., Schwartz, M. J., and Sheese, P. E.: MIPAS temperature from the stratosphere to the lower thermosphere: Comparison of vM21 with ACE-FTS, MLS, OSIRIS, SABER, SOFIE and lidar measurements, *Atmospheric Measurement Techniques*, 7, 3633–3651, doi:10.5194/amt-7-3633-2014, <https://www.atmos-meas-tech.net/7/3633/2014/>, 2014.
- 525 Hauchecorne, A., Blanot, L., Wing, R., Keckhut, P., Khaykin, S., Bertaux, J.-L., Meftah, M., Claud, C., and Sofieva, V.: A new MesosphEO dataset of temperature profiles from 35 to 85 km using Rayleigh scattering at limb from GOMOS/ENVISAT daytime observations, *Atmospheric Measurement Techniques Discussions*, 2018, 1–19, doi:10.5194/amt-2018-241, <https://www.atmos-meas-tech-discuss.net/amt-2018-241/>, 2018.
- 530 Hoppel, K. W., Baker, N. L., Coy, L., Eckermann, S. D., McCormack, J. P., Nedoluha, G. E., and Siskind, E.: Assimilation of stratospheric and mesospheric temperatures from MLS and SABER into a global NWP model, *Atmospheric Chemistry and Physics*, 8, 6103–6116, 2008.
- 535 Johnson, K. W. and Gelman, M. E.: Trends in upper stratospheric temperatures as observed by rocketsondes (1965–1983), *International Council of Scientific Unions Handbook for MAP*, 18, 1985.
- Leblanc, T., McDermid, I. S., Hauchecorne, A., and Keckhut, P.: Evaluation of optimization of lidar temperature analysis algorithms using simulated data, *Journal of Geophysical Research: Atmospheres*, 103, 6177–6187, doi:10.1029/97JD03494, <https://agupubs.onlinelibrary.wiley.com/doi/abs/10.1029/97JD03494>, 1998.
- 540 Leblanc, T., Sica, R. J., Van Gijssel, J. A. E., Godin-Beekmann, S., Haefele, A., Trickl, T., Payen, G., and Gabarrot, F.: Proposed standardized definitions for vertical resolution and uncertainty in the NDACC lidar

- ozone and temperature algorithms – Part 1: Vertical resolution, *Atmospheric Measurement Techniques*, 9, 4029–4049, doi:10.5194/amt-9-4029-2016, <https://hal-insu.archives-ouvertes.fr/insu-01306586>, 2016.
- Leblanc, T., Sica, R. J., van Gijssel, J. A. E., Haefele, A., Payen, G., and Liberti, G.: Proposed standardized definitions for vertical resolution and uncertainty in the NDACC lidar ozone and temperature algorithms - Part 3: Temperature uncertainty budget, *Atmospheric Measurement Techniques*, 9, 4079–4101, doi:10.5194/amt-9-4079-2016, 2016.
- Licel: Licel Data Sheet Kernel Description, <https://http://licel.com/transdat.htm#DNL>, 2018.
- Livesey, N. J., Snyder, W. V., Read, W. G., and Wagner, P. A.: Retrieval algorithms for the EOS Microwave limb sounder (MLS), *IEEE Transactions on Geoscience and Remote Sensing*, 44, 1144–1155, doi:10.1109/TGRS.2006.872327, 2006.
- Meek, C. E., Manson, A. H., Hocking, W. K., and Drummond, J. R.: Eureka, 80° N, SKiYMET meteor radar temperatures compared with Aura MLS values, *Annales Geophysicae*, 31, 1267–1277, doi:10.5194/angeo-31-1267-2013, <https://www.ann-geophys.net/31/1267/2013/>, 2013.
- Mertens, C. J., Mlynczak, M. G., López-Puertas, M., Wintersteiner, P. P., Picard, R. H., Winick, J. R., Gordley, L. L., and Russell, J. M.: Retrieval of mesospheric and lower thermospheric kinetic temperature from measurements of CO₂ 15 μm Earth Limb Emission under non-LTE conditions, *Geophysical Research Letters*, 28, 1391–1394, doi:10.1029/2000GL012189, <http://dx.doi.org/10.1029/2000GL012189>, 2001.
- Pautet, P.-D., Taylor, M. J., Pendleton, W. R., Zhao, Y., Yuan, T., Esplin, R., and McLain, D.: Advanced mesospheric temperature mapper for high-latitude airglow studies, *Appl. Opt.*, 53, 5934–5943, doi:10.1364/AO.53.005934, <http://ao.osa.org/abstract.cfm?URI=ao-53-26-5934>, 2014.
- Remsberg, E. E., Marshall, B. T., Garcia-Comas, M., Krueger, D., Lingenfelter, G. S., Martin-Torres, J., Mlynczak, M. G., Russell, J. M., Smith, A. K., Zhao, Y., Brown, C., Gordley, L. L., Lopez-Gonzalez, M. J., Lopez-Puertas, M., She, C.-Y., Taylor, M. J., and Thompson, R. E.: Assessment of the quality of the Version 1.07 temperature-versus-pressure profiles of the middle atmosphere from TIMED/SABER, *Journal of Geophysical Research: Atmospheres*, 113, doi:10.1029/2008JD010013, <http://dx.doi.org/10.1029/2008JD010013>, d17101, 2008.
- Schwartz, M. J., Lambert, A., Manney, G. L., Read, W. G., Livesey, N. J., Froidevaux, L., Ao, C. O., Bernath, P. F., Boone, C. D., Cofield, R. E., Daffer, W. H., Drouin, B. J., Fetzer, E. J., Fuller, R. A., Jarnot, R. F., Jiang, J. H., Jiang, Y. B., Knosp, B. W., Krüger, K., Li, J. F., Mlynczak, M. G., Pawson, S., Russell, J. M., Santee, M. L., Snyder, W. V., Stek, P. C., Thurstans, R. P., Tompkins, A. M., Wagner, P. A., Walker, K. A., Waters, J. W., and Wu, D. L.: Validation of the Aura Microwave Limb Sounder temperature and geopotential height measurements, *Journal of Geophysical Research: Atmospheres* (1984–2012), 113, doi:10.1029/2007JD008783, <http://dx.doi.org/10.1029/2007JD008783>, 2008.
- Siva Kumar, V., Rao, P. B., and Krishnaiah, M.: Lidar measurements of stratosphere-mesosphere thermal structure at a low latitude: Comparison with satellite data and models, *Journal of Geophysical Research: Atmospheres*, 108, doi:10.1029/2002JD003029, <http://dx.doi.org/10.1029/2002JD003029>, 4342, 2003.
- Sivakumar, V., Prasanth, P. V., Kishore, P., Bencherif, H., and Keckhut, P.: Rayleigh LIDAR and satellite (HALOE, SABER, CHAMP and COSMIC) measurements of stratosphere-mesosphere temperature over a southern sub-tropical site, Reunion (20.8° S; 55.5° E): climatology and comparison study, *An-*

nales Geophysicae, 29, 649, <https://www.lib.uwo.ca/cgi-bin/ezpauthn.cgi?url=http://search.proquest.com/docview/869915562?accountid=15115>, 2011.

585 Taori, A., Dashora, N., Raghunath, K., Russell, J. M., and Mlynczak, M. G.: Simultaneous mesosphere-thermosphere-ionosphere parameter measurements over Gadanki (13.5°N, 79.2°E): First results, *Journal of Geophysical Research: Space Physics*, 116, doi:10.1029/2010JA016154, <http://dx.doi.org/10.1029/2010JA016154>, a07308, 2011.

Taori, A., Jayaraman, A., Raghunath, K., and Kamalakar, V.: A new method to derive middle atmospheric temperature profiles using a combination of Rayleigh lidar and O₂ airglow temperatures measurements, *Annales Geophysicae*, 30, 27–32, doi:10.5194/angeo-30-27-2012, 2012a.

590 Taori, A., Kamalakar, V., Raghunath, K., Rao, S., and Russell, J.: Simultaneous Rayleigh lidar and airglow measurements of middle atmospheric waves over low latitudes in India, *Journal of Atmospheric and Solar-Terrestrial Physics*, 78–79, 62–69, doi:10.1016/j.jastp.2011.06.012, 2012b.

Waters, J. W., Froidevaux, L., Harwood, R. S., Jarnot, R. F., Pickett, H. M., Read, W. G., Siegel, P. H., Cofield, R. E., Filipiak, M. J., Flower, D. A., Holden, J. R., Lau, G. K., Livesey, N. J., Manney, G. L., Pumphrey, H. C., Santee, M. L., Wu, D. L., Cuddy, D. T., Lay, R. R., Loo, M. S., Perun, V. S., Schwartz, M. J., Stek, P. C., Thurstans, R. P., Boyles, M. A., Chandra, K. M., Chavez, M. C., Chen, G.-S., Chudasama, B. V., Dodge, R., Fuller, R. A., Girard, M. A., Jiang, J. H., Jiang, Y., Knosp, B. W., LaBelle, R. C., Lam, J. C., Lee, K. A., Miller, D., Oswald, J. E., Patel, N. C., Pukala, D. M., Quintero, O., Scaff, D. M., Snyder, W. V., Tope, M. C., Wagner, P. A., and Walch, M. J.: The Earth observing system microwave limb sounder (EOS MLS) on the aura Satellite, *IEEE Transactions on Geoscience and Remote Sensing*, 44, 1075–1092, doi:10.1109/TGRS.2006.873771, 2006.

605 Wing, R., Hauchecorne, A., Keckhut, P., Godin-Beekmann, S., Khaykin, S., McCullough, E. M., Mariscal, J.-F., and d’Almeida, E.: Lidar temperature series in the middle atmosphere as a reference data set – Part 1: Improved retrievals and a 20-year cross-validation of two co-located French lidars, *Atmospheric Measurement Techniques*, 11, 5531–5547, doi:10.5194/amt-11-5531-2018, <https://www.atmos-meas-tech.net/11/5531/2018/>, 2018.

Wuebbles, D., Fahey, D., and Hibbard, K.: The Climate Science Special Report (CSSR) of the Fourth National Climate Assessment (NCA4), in: *AGU Fall Meeting Abstracts*, 2016.

610 Xu, J., She, C. Y., Yuan, W., Mertens, C., Mlynczak, M., and Russell, J.: Comparison between the temperature measurements by TIMED/SABER and lidar in the midlatitude, *Journal of Geophysical Research: Space Physics*, 111, doi:10.1029/2005JA011439, <http://dx.doi.org/10.1029/2005JA011439>, a10S09, 2006.

615 Yuan, T., She, C.-Y., Krueger, D., Reising, S. C., Zhang, X., and Forbes, J.: A collaborative study on temperature diurnal tide in the midlatitude mesopause region (41N, 105W) with Na lidar and TIMED/SABER observations, *Journal of Atmospheric and Solar-Terrestrial Physics*, 72, 541–549, doi:10.1016/j.jastp.2010.02.007, 2010.

Yue, C., Yang, G., Wang, J., Guan, S., Du, L., Cheng, X., and Yang, Y.: Lidar observations of the middle atmospheric thermal structure over north China and comparisons with TIMED/SABER, *Journal of Atmospheric and Solar-Terrestrial Physics*, 120, 80–87, doi:10.1016/j.jastp.2014.08.017, 2014.